

A low complexity contextual stacked ensemble-learning approach for pedestrian intent prediction

Chia-Yen Chiang, Yasmin Fathy, Gregory Slabaugh, Mona Jaber

Abstract—Walking as a form of active travel is essential in promoting sustainable transport. It is thus crucial to accurately predict pedestrian crossing intention and avoid collisions, especially with the advent of autonomous and advanced driver-assisted vehicles. Current research leverages computer vision and machine learning advances to predict near-misses; however, this often requires high computation power to yield reliable results. In contrast, this work proposes a low-complexity ensemble-learning approach that employs contextual data for predicting the pedestrian’s intent for crossing. The pedestrian is first detected, and their image is then compressed using skeleton-ization, and contextual information is added into a stacked ensemble-learning approach. Our experiments on different datasets achieve similar pedestrian intent prediction performance as the state-of-the-art approaches with 99.7% reduction in computational complexity. Our source code and trained models will be released upon paper acceptance

Index Terms—pedestrian detection, pedestrian intent, feature extraction, ensemble-learning, computational complexity

I. INTRODUCTION

ACTIVE mobility is a critical component in the pathway to sustainable and effective urban transportation systems. Active travel is a transportation mode in which people travel from one place to another by being physically active, such as walking or cycling. However, the growing concerns about the safety of vulnerable road users (VRUs), such as pedestrians, have slowed the uptake of active travel. According to the World Health Organisation data, 1.19 million people die each year as a result of road traffic crashes and more than half are VRUs¹.

The near future vision of urban mobility consists of various modes of transport sharing the open urban space and road network including VRUs, driver-assisted, and driverless vehicles [1]. Human drivers have ‘common sense’ that allows them to ‘read’ a scene, predict the behavior of VRUs, and communicate with them through eye contact to indicate safety to crossing [2]. Can we train autonomous vehicles to develop a similar ‘common sense’ that predicts the behavior of VRUs? Pedestrian intent prediction (PIP) has gained increased attention in recent years, with significant progress being made in autonomous vehicles as a part of the intelligent transportation systems paradigm.

PIP methods often build on technologies for connected and autonomous vehicles (CAVs) and leverage a spectrum of sensors (e.g., radar, LIDAR, optical cameras, and ultrasonic sensors) with different machine learning (ML) methods to automate decisions that avoid collisions [3]. Among these sensors, cameras provide the most detailed depiction of the vehicle’s surroundings, and the advances in related computer vision approaches allow for precise localization of pedestrians and PIP. However, camera-based data is often complex, requiring high computation power for processing. Furthermore, this data carries personal information about pedestrians that might put them at risk if misused while being irrelevant in solving the PIP problem.

There are two dominant approaches for computer vision (CV)-enabled PIP: the first is based on cameras installed along the roads, and the second relies on car-mounted cameras. The former relies on fixed cameras; thus, they require reliable broadband connectivity to the cloud server, which has high computational power and storage [4]. Other work leverages edge computing to offload pedestrian-related prediction tasks and ensure reliability [5]. Privacy concerns arise when data containing personal information (e.g., people’s faces) is sent over the network for processing. The second dominant approach for enabling PIP is based on collecting and processing data from vehicle-mounted cameras and other sensory devices that are key enablers for developing the advanced driver-assistance system (ADAS) and automated driving technologies. With the advent of 5G and next-generation networks, broadband connectivity is possible for moving vehicles but is less reliable and more costly than the connectivity of fixed cameras [6]. The processing power available to ADAS is less limited than road-based cameras, but the robustness of the sensors, data fusion, and AI algorithms varies significantly between different vendors. It follows that centralized learning is still preferred to ensure the reliability of the AI models. Therefore, data communication to the central server is predominant even in this approach and suffers from the challenge of transferring large volumes of data [7].

Another rising concern common to both approaches stems from their heavy dependency on computationally complex AI models and the contribution of these to greenhouse gas emissions. This is underscored in [8] in which computational researchers are solicited to monitor and report the carbon footprint of their work to ensure a more sustainable future. The relation between computational complexity and carbon footprint is highlighted in [9] which acknowledges the irrefutable role of AI in enabling sustainable futures while it advocates

C. Chiang, G. Slabaugh and M. Jaber are with the School of Electronic Engineering & Computer Science, Queen Mary University of London: {c.chiang, g.slabaugh, m.jaber}@qmul.ac.uk. Y. Fathy is with the Department of Engineering, University of Cambridge yafa2@cantab.ac.uk

¹<https://www.who.int/news-room/fact-sheets/detail/road-traffic-injuries>

for effective low-complexity AI models.

Recent research [10] [11] [7] proposes Graph Neural Networks to model the change of human keypoints in time to represent pedestrian crossing behavior. Others [12] employ Long Short-Term Memory (LSTM) to model the relationship between pedestrian locations and crossing behavior. A transformer network is proposed in [13] for PIP to capture the AI uncertainty in scene complexities. Despite the incremental improvements in PIP performance in these works, it often comes at the cost of higher computational complexity and greater impact on greenhouse gas emissions.

This work proposes a new Contextual Stacked Ensemble-learning (CSE) method for solving PIP using car-based cameras. Similar to [10] [11] [7], we use skeleton-ization, which compresses the image of a pedestrian to 17 keypoints, thus reducing the volume of the camera-based data by 4336 times (see Section IV-B1) while addressing privacy concerns. As an outcome, transmitting the skeleton-ized data to the cloud server for further processing and conducting a deep intent prediction becomes feasible. The main goals of the proposed method are threefold: data compression and privacy, robust and reliable PIP, and low computational complexity. The robust and reliable PIP model is achieved by leveraging contextual information (e.g., categorical data describing the scene and pedestrian trajectory) with stacked ensemble learning. The proposed CSE approach achieves comparable PIP performance to state-of-the-art work with a step reduction in complexity (99.99% reduction in FLOPS and 99.7% less trainable parameters). Our approach received the first prize award of the IEEE Intelligent Transportation Systems Society (ITSS) Student Competition in Pedestrian Behavior Prediction [14].

II. PROBLEM FORMULATION

In this work, the PIP problem is formulated as predicting the behavior of a pedestrian as *Crossing* or *Not-Crossing* based on video clips taken from the front of a vehicle. Each video clip, denoted as \mathbb{S}_v , for $v \in \{1, \dots, V\}$ (V is the total number of clips in the dataset), contains a consecutive set of M frames F_i , where i is the index of frames $i \in \{1, \dots, M\}$. Each clip \mathbb{S}_v includes a maximum of P bounding boxes (*bbx*), and each *bbx* frames a single pedestrian with an index j and may include other pedestrians in the background (i.e., not labeled). It follows that each annotated clip includes the labeled behavior of P pedestrians with a unique index $j \in \{1, \dots, P\}$. Given the one-to-one mapping between *bbx* and pedestrians, the same index j is used to reference the *bbx* that frames a pedestrian with index j . In each video clip \mathbb{S}_v , a pedestrian with index $j \in \{1, \dots, P\}$ (and the *bbx* that frames them) is annotated with a label y ; $y = 1$ *Crossing* if pedestrian intends to cross a street at any point in \mathbb{S}_v or $y = 0$ for (*Not-Crossing* or *Irrelevant*, i.e., without a behavioral label) otherwise.

The data in each video clip is analysed from two perspectives. The first relates to the pedestrian and is based on sliding widows of 32 frames that span the full video clip. Two data streams are extracted from this perspective: keypoints that represent the pose of the pedestrian (see Section IV-B1) and the pedestrian's trajectory relative to the

frame (see Section IV-B3). The other perspective captures the contextual information from two angles: global context and local context. The former is common to all pedestrians in a given frame and describes the speed of the ego-vehicle, the status of the traffic light it faces, and the road type it drives on. The latter is specific to each pedestrian and describes their relative local context such as standing at an intersection (see Section IV-B2). The goal of this work is therefore to classify sliding windows as positive (*Crossing*) or negative (*Not-Crossing* and *Irrelevant*) case.

III. METHODOLOGY

Different methods have been proposed to address PIP in [7], [15] [16], [17] however, these methods fail to examine class performance or suffer from high computational complexity. Therefore, in this work, we propose Contextual Stacked Ensemble (CSE), a novel ensemble learning system that builds on three individual models which we introduce in this section. The first model, M1, consists of a graph neural network (GNN) model for classifying skeleton-ized data, \mathbb{K}_v as *Crossing/Not-Crossing*. The second model, M2, employs stacked gated recurrent network units (GRUs) for solving PIP using time-series and categorical data from JAAD's vehicle and traffic annotations. The third model, M3, employs a one-dimensional convolutional neural network for solving PIP based on a pedestrian's trajectory, τ_v . The CSE combines these three models as shown in Figure 5 (right). For comparison, two models are also implemented using a similar structure. The entire ensemble learning system is thus structured as Figure 1 with detailed explanations of each of its three models (M1, M2, M3) in the following subsections.

A. M1: Graph Neural Network

The GNN model (M1) is used to classify a sequence of graphs in which the vertices describe the K_{max} keypoints in the frame with index i and are represented by the matrix \mathcal{K}_i which is obtained through the skeleton-ization process; in this case, $k_\kappa = \{w_\kappa, h_\kappa\}$ represents the relative position of a keypoint with index κ and \mathbb{K}_v represents the sequence of matrices \mathcal{K}_i during the video clip \mathbb{S}_v .

$$\mathcal{K}_i = [k_1, \dots, k_\kappa], \kappa = \{1, \dots, K_{max}\} \quad (1)$$

$$k_\kappa = \{w_\kappa, h_\kappa\} \mid 0 < w_\kappa < W; 0 < h_\kappa < H \quad (2)$$

$$\mathbb{K}_v = \{\mathcal{K}_i : 1 \leq i \leq F_{max}\} \quad (3)$$

These keypoints (vertices) are connected with a fixed adjacency matrix \mathcal{A} defined to represent the connectivity between any two different keypoints k_o and k_q in a skeleton, such that $A(o, q) = 1$ when these are connected (e.g. head and neck) [15].

$$\mathcal{A} = [\{A(1, 1), \dots, A(1, K_{max})\}, \dots, \{A(\kappa, 1), \dots, A(\kappa, K_{max})\}, \dots, \{A(K_{max}, 1), \dots, A(K_{max}, K_{max})\}] \quad (4)$$

The model consists of a convolutional block, a skip connection and a GRU, as shown in Figure 2. The input keypoints are first applied matrix multiplication with a normalized adjacency

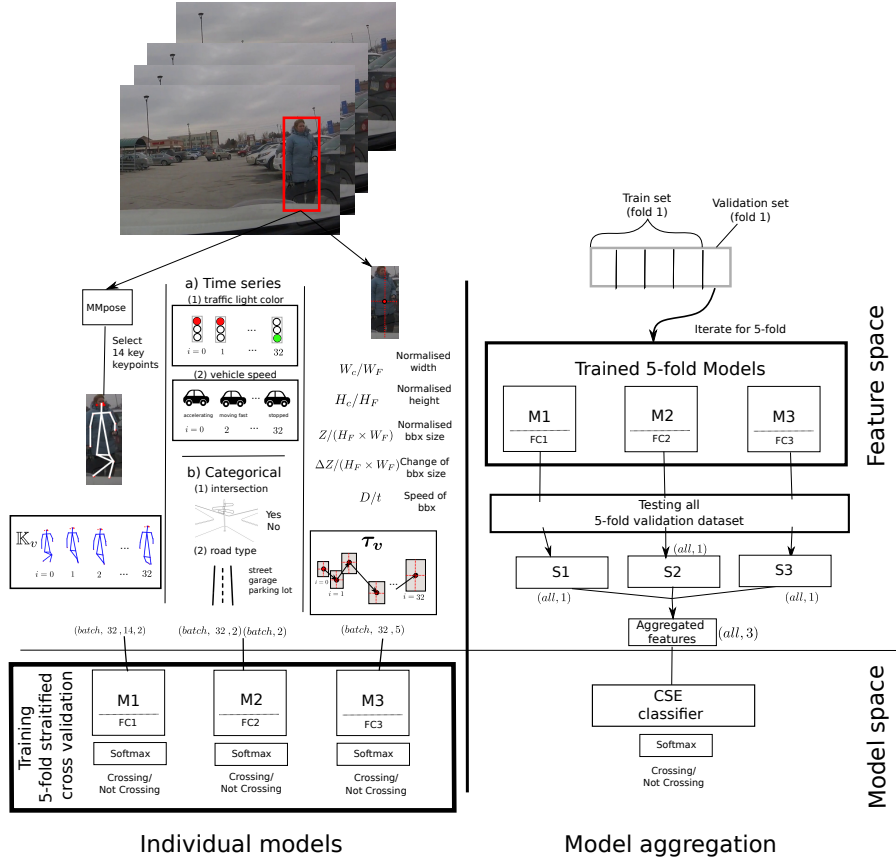


Fig. 1. Our proposed CSE framework is composed of a stacked ensemble classifier and three models for PIP classification. (Top-left) Data preprocessing on video frames shows how three representations are extracted from the raw video. (Bottom-left) M1 uses skeleton-ization for data compression followed by a Graph Neural Network. M2 uses contextual data and a Gated Recurrent Unit network. M3 extracts the relative location of the pedestrian and uses a one-dimensional convolutional neural network. (Top-right and bottom-right) The aggregated features stack the output of the last fully connected (FC) layer, i.e., S1, S2, S3, from the three models by aggregating testing results from 5-fold validation of their corresponding model, i.e., M1, M2, M3. The system then produces prediction results from the contextual stacked ensemble classifier.

matrix. The matrix product involves summing up keypoint features from adjacent nodes. The summed-up features of each node are embedded into a convolutional layer for further feature extraction. To prevent shrinking feature maps, the convolutional layer must use “same” padding. A dropout (0.5) layer is then used to encourage model generalization.

The skip connection operation adds input keypoints to the dropout output. By passing coming layers and preserving early layer information, the model can keep both low and high level representations, thus improves feature learning. A 1×1 convolution on the skip connection branch adjusts the channel dimension to enable the addition to the features output by the 2D convolutional block.

Finally, a GRU layer is used to model the evolution of keypoint features in the time domain. The hidden size is set to 16. The last hidden output is then fed to a fully-connected layer for *Crossing/Not-Crossing* classification.

M2: Stacked Gated Recurrent Unit Network

Inspired by the stacked GRU in [18], we apply the stacked GRU in modelling time-series and categorical contextual information from the vehicle and traffic background as shown in Figure 3. The stacked GRUs model (M2) iterates each time-series data and feeds it in a GRU with only one layer to produce all hidden outputs from frame F_1 to F_{max} . Before feeding all hidden outputs to the next GRU, a next time-series data is merged with the hidden outputs. The output of the last GRU is the last hidden output instead of a full sequence of hidden outputs.

Specifically, the categorical data used for contextual information in M2 consists of the following data (Figure 3):

- Data 1 (time-series data over the duration of F_{max} frames) - vehicle speed $\{Stopped, Slow, Fast, Accelerating, Decelerating\}$: A pedestrian is less likely to cross if they notice an upcoming vehicle that is speeding.
- Data 2 (time-series data over the duration of F_{max} frames) - Traffic signal status $\{Red, Green\}$: A pedestrian

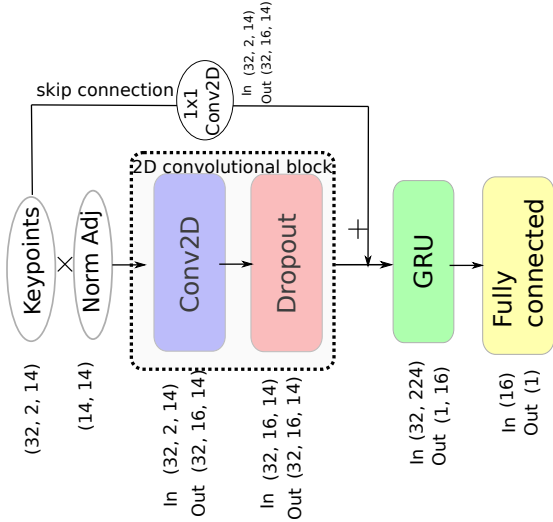


Fig. 2. **M1**: The figure shows model structure with input and output dimension in each model block.

is less likely to cross the street if the traffic signal controlling the passing vehicles is green; in which case the pedestrian signal would be red.

- Data 3 (categorical with one value for each bbx)- Is the pedestrian standing at an intersection? $\{Yes, No\}$: A pedestrian waiting at an intersection is likely to cross the street.
- Data 4- (categorical with one value for each video)- Type of road $\{Garage, Parking\ lot, Street\}$: It is more likely that a pedestrian seen on the street might cross than a pedestrian standing/walking in a parking lot.

Our proposed approach is different from [18] in the following. The last hidden output of stacked GRUs in the proposed M2 is concatenated with categorical data. The combined features then are projected to a fully connected layer before *Crossing/Not-Crossing* classification (see Figure 3).

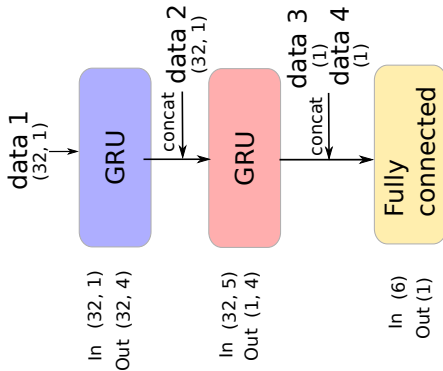


Fig. 3. **M2**: a stacked GRUs is used to model contextual information that can affect crossing decision.

B. M3: 1D convolutional Neural Network

For modelling the relationship between pedestrian trajectory τ_v and PIP decision, a shallow 1D-CNN (M3) is proposed (see Figure III-B). 1D-CNN is often used to predict a future

trajectory given historical data [19], [20] while [21] uses both RNN and CNN to predict future classes of an encoded trajectory. Trajectories possess not only pedestrian speed, direction, and pedestrian depth information but are also strongly related to PIP decisions. We, therefore, adopt a 1D-CNN for M3 to solve PIP based on past trajectory as contextual information. Our proposed 1D-CNN model contains only three layers: a convolutional layer for extracting 1D time-series features, a dropout layer for preventing overfitting, and a fully connected layer for PIP classification, as shown in Figure III-B.

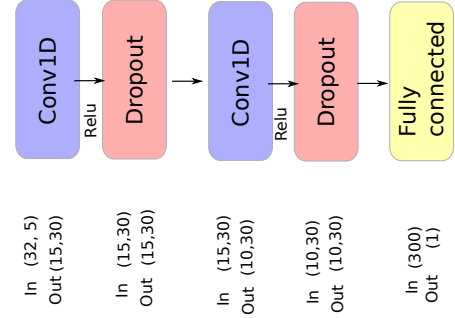


Fig. 4. **M3**: A 1D-CNN could be used to predict future trajectory given historical data. The five inputs of the trajectory are introduced in Section IV-B3.

C. CSE: Contextual Stacked Ensemble

Similar to the approach used in [22] for multimodal feature fusion, we propose a stack-ensemble learning method to fuse features from each of the three models defined above. Each of M1, M2, and M3 is trained by a five-fold stratified cross-validation with a fixed sampling seed 1. The variant of cross-validation ensures each fold preserves the same class ratio. The last fully connected layer of each of the three models M1, M2, and M3 produces an output S1, S2, or S3, respectively (as shown in Figures 5 and 1) when the test input is a five-fold validation dataset. We then concatenated S1, S2, S3 to form the aggregated features that are then fed into a CSE classifier to boost overall prediction. The classifier is then followed by a softmax and an argmax function to generate the final *Crossing/Not-Crossing* classification results (see CSE model structure in Figure 5).

IV. EXPERIMENTS

We conducted the experiments of our proposed method on two datasets: (1) Joint Attention in Autonomous Driving (JAAD) dataset [23] as described in Section IV-A. Next, we introduce the data preprocessing, where sequences of frames are processed, and three different features related to pedestrians are extracted. The first is keypoint representation of pedestrians in bbx (Section IV-B1). The second consists of contextual information around this pedestrian including time-series data and categorical data (Section IV-B2). The last is the historical trajectory of the pedestrian, which is extracted by analyzing the changing position of the bounding box with respect to the frame (Section IV-B3).

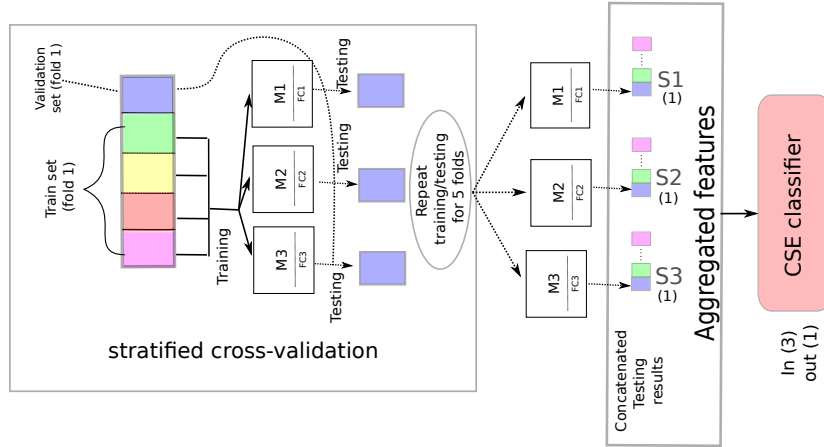


Fig. 5. **CSE**: Model structure of Contextual Stacked Ensemble learning. In stratified cross-validation, we first train models with five-fold training datasets. An example is shown in Fold 1, where three models are trained on four blocks (see bottom-to-top 4 blocks marked train set Fold 1 above). In this case, the validation block (top purple) is used to test each of the three models. This process is repeated with the iteration of folds; for instance, the next fold would use the green block for validation and train using the remaining blocks. The testing results of all five folds are concatenated to form S1, S2, and S3 as an input of CSE classifier.

A. Dataset description

In this work, we use the Joint Attention in Autonomous Driving (JAAD) Dataset [23], which is richly annotated and contains $V = 346$ video clips (each is around five to ten seconds long) extracted from over 240 hours of driving footage from dash cameras positioned at the front of the car. The dataset provides frame-wise, distinct labels such as pedestrian reaction toward drivers, pedestrians’ demographic attributes, and traffic conditions, which are not found in other datasets, such as the Multiple Object Tracking (MOT) Challenge ². There are two versions of the same dataset, JAADbeh and JAADall, where JAADbeh is a subset of JAADall, and the latter includes additional annotations of pedestrians in the background. ³.

B. Data preprocessing

1) *skeleton-ization*: The first data representation aims to capture the pose of a pedestrian by examining the essential keypoints of the human body following a skeleton-ization approach. The reasoning behind this representation is multifaceted. First, it avoids the capturing of personal information (e.g., face, hair, clothing, etc.) while retaining the essential information for pose analysis and, therefore, action prediction. Second, reducing the complexity of the data representation decreases the computational requirement for classification, which indicates that this task can be conducted at the edge with limited processing power. Third, given that the data is significantly compressed with skeleton-ization, it is then possible to efficiently transfer data to the central server for further processing. We obtain 17 keypoints for each pedestrian by adopting a MMpose [24] as shown in Figure IV-B1. MMpose is a powerful open source toolbox that provides

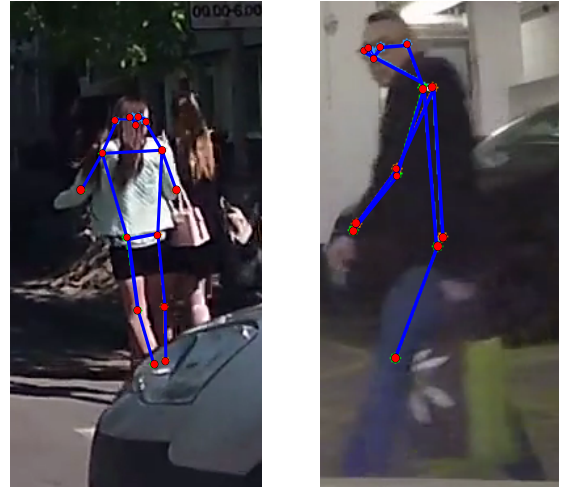


Fig. 6. The MMpose returns 17 keypoints for each *bbx*. (Left) *Not-Crossing* (right) *Crossing*

weights from more than 200 networks for human keypoint detection.

To obtain 17 keypoints, each sequence of F_{max} *bbxs* represents a data sample (i.e., a pedestrian) and is labeled as *Crossing* if any *bbx* found in frame F_i ($1 \leq i \leq F_{max}$) is categorised as such, otherwise, it is labeled as *Not-Crossing*.

2) *Contextual data*: There is a plethora of information available to connected vehicles (see Section I) that can be inferred from the sensors or location-based services.

In this section, we examine key attributes and investigate if this additional information (discussed in Section I) is more likely to improve the prediction of pedestrians (*Crossing/Not Crossing*) in the PIP problem. There are three categories of attributes that can be obtained:

- Pedestrian Behavior shown in Figure 7 and includes **Action**={*Walking, Standing*}, **Hand Gesture**={*Greet, Yield, Rightofway, other*}, **Reaction**={*Slow-down, Speed-up*,

²<https://motchallenge.net>

³JAADall dataset incorporates all non-labeled pedestrians in JAADbeh by manually annotating these to *Not-Crossing* class. (see details in Section IV-B)

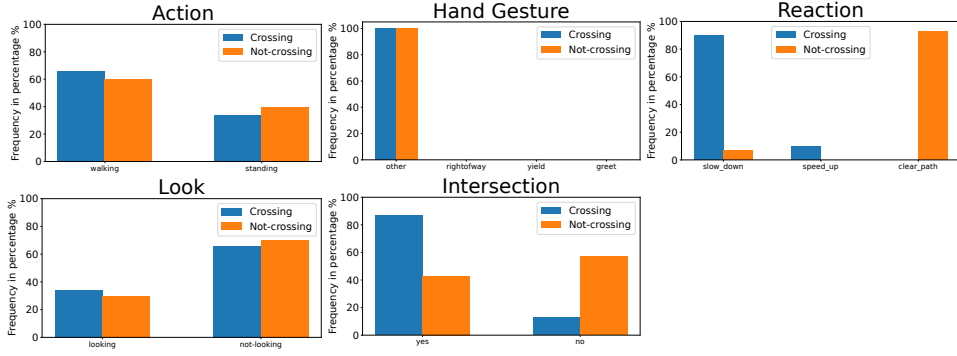


Fig. 7. Pedestrian Behavior comparison between *Crossing* and *Not-Crossing* before crossing action. Intersection and Reaction have the most distinguishable patterns in subcategories for both classes.

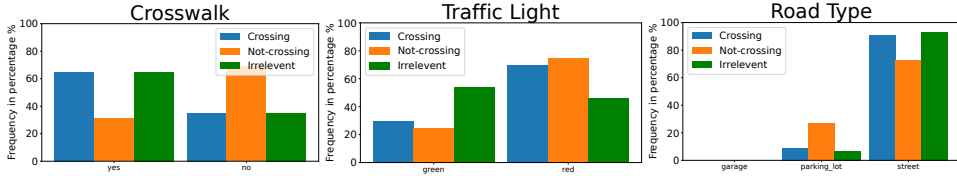


Fig. 8. Traffic Annotation comparison between *Crossing*, *Not-Crossing* and *Irrelevant*. It is clear that *Irrelevant* has similar patterns with *Crossing* in Pedestrian Crossing, and Road type. In addition, Traffic Light can't differentiate *Crossing* and *Not-crossing* but Pedestrian Crossing and Road Type can.

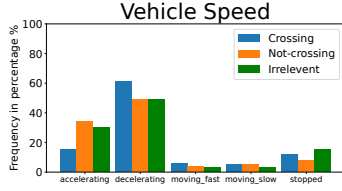


Fig. 9. Vehicle Speed comparison between *Crossing*, *Not-Crossing* and *Irrelevant* before crossing action. Vehicle speed seems to differentiate *Crossing* with the group of *Not-crossing* and *Irrelevant*.

Clear-path}, *Look*={*Yes*, *No*}, and *Intersection*={*Yes*, *No*}. All except *Intersection* are time-series data.

- Traffic Background shown in Figure 8 and includes **Crosswalk** (or Pedestrian Crossing)={*Yes*, *No*}, **Traffic Light**={*Green*, *Red*}, and **Road Type**={*Garage*, *Parking lot*, *Street*). All except **Road Type** are time-series data.
- Vehicle speed before pedestrian's crossing action shown in Figure 9

Pedestrians that are not labeled as *Crossing* or *Not-Crossing* have been marked as *Irrelevant* in Figures 7, 8, and 9.

It may be counter-intuitive at first that some of the **Pedestrian Behavior** attributes shown in Figure 7 do not have a distinct pattern for *Crossing* or *Not-Crossing*. For instance, pedestrians that are *looking* and those that are *walking* are more likely to cross but the distinction with the *Not-Crossing* category is minimal. Careful analysis indicates that pedestrians who *stand* may have the intention to cross and those who *look* may be standing-by. *Reaction* shows that *Crossing* pedestrians are more likely to slow down while *Not-Crossing* are more likely to clear path. *Intersection* shows that *Crossing* pedestrians are likely to stand on the intersection.

Examining the **Traffic Annotation** attributes can similarly

be misleading where the occurrences of the two classes *Crossing*, and *Irrelevant* with each of the attributes *Road Type* or *Crosswalk* and is almost identical. As such, it is not possible to distinguish between these two classes by examining these attributes.

Pedestrians that are labeled as *Irrelevant* are more likely to be seen in the traffic scene when the traffic light is green than the other two classes. Following careful investigation of such occurrences, we noted in most cases the pedestrians are not on the same lane as the ego-vehicle. Instead, they could be on the zebra crossing parallel to the ego-vehicle's lane or they could be on the sidewalks.

Further examining the **Traffic Annotation** attributes in Figure 8, we can see *Crossing* pedestrians are more likely to appear in the traffic scene with *Crosswalk* (Pedestrian Crossing) and on the *Street* rather than in *Garage*, comparing to *Not-Crossing*. As for **Vehicle Speed** attribute in Figure 9, it is intuitive to note that vehicles *Decelerate* at the sight of pedestrians irrelevant of what their PIP. However, they are more likely to *Decelerate* in front of *Crossing* pedestrians and likely to *Stop* when facing *Crossing* and *Irrelevant* pedestrians.

3) *Pedestrian trajectory*: The trajectory of the pedestrian within each given frame carries contextual information that can be useful in solving the PIP problem. The location of the pedestrian is equated to the relative position of *bbx* with respect to the frame. In this work, we calculate the relative position of the central *bbx* pixel located at $[W_c = W/2, H_c = H/2]$, where W and H are the width and height of the *bbx*. The pedestrian's depth, Z , is inferred from the size of the *bbx* where a small value indicates that the *bbx* is far away from the camera and vice-versa. Knowing that the absolute coordinates (W_c, H_c) and the size Z can be biased by different

frame sizes, we normalize the values such that the pedestrian normalized location is $(W_c/W_F, H_c/H_F)$ and the normalized size is $Z/(H_F \times W_F)$, where H_F is the height of the frame and W_F is the width. In addition, we calculate the change of normalized size over time $\Delta Z/(H_F \times W_F)$ as well as the speed of movement, which was estimated by getting the ratio of the normalized traveled distance over time.

For each video clip \mathbb{S}_v , the normalized positioning vector $q_{v,i} = [W_{c_i}/W_F, H_{c_i}/H_F, Z_i/(H_F \times W_F), \Delta Z/(H_F \times W_F), D/t]$ of each *bbx* containing a pedestrian in frames F_i ($i = [0, \dots, F_{max}]$) is calculated. Thus, the trajectory of a pedestrian in video clip \mathbb{S}_v is represented by τ_v .

C. Results and Discussion

We address the problem of pedestrian intention prediction, predicting label \hat{y} for each given input sliding window \mathbb{W}_v (32 frames) sampled from each video clip \mathbb{S}_v . In preparation for the model training and testing, we split the dataset to train/val/test subsets based on JAAD’s suggestion. The JAAD’s train and validation were then merged before splitting again for stratified 5-fold cross-validation [26]. For each fold, the method preserves the percentage of *Crossing* and *Not-Crossing* data points instead of random sampling on the positive ($y = 1$, *Crossing*) and negative ($y = 0$, *Not-Crossing*, *Irrelevant*) samples pool. This approach ensures that the training performance of each fold is not biased by a random ratio of classes and preserves all information in the samples. The stratified 5-fold crossing validation was used only in training models on JAADbeh. This method preserves the class ratio and therefore, ensures the training stability, which works well for JAADbeh. However, with an extreme class distribution, such as JAADall, we find that models perform better when classes are balanced. Therefore, we create a customized 5-fold dataset in which each fold has all positive samples from the merged data and randomly selected negative samples (without replacement) from the merged data to match the number of positive samples. Nonetheless, the test results are derived using the test dataset defined in ⁴ for both JAADbeh and JAADall.

Each of the three data streams described in Section IV-B is used independently to train three different models, M1, M2, and M3, as shown in Figure 1. An ensemble learning approach is built based on the feature representation of these models to form the proposed CSE. We first present the results of each model in isolation in addition to the CSE in Table I and compare the performance and complexity of these to the state-of-the-art models. As seen in Table I, our proposed CSE using M1, M2, and M3 delivers the best F1 score, outperforming the next best models, Pedgraph+ [7] and Faster PCPNet [10], by 3% at a much lower computational complexity. Our model requires 331 times less FLOPS than Pedgraph+ and 10000 less than Global PCPA; moreover, our model consists of 5.2 times less trainable parameters than Pedgraph+ and 4500 times less than Global PCPA. Recall is an important metric as it reflects the ability of the model to detect *Crossing*; our model ranks second to Global PCPA [25] with 4% reduction in recall

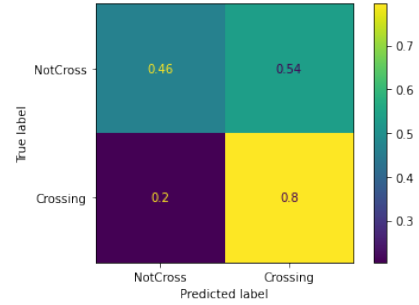


Fig. 10. CSE confusion matrix for JAADbeh

and 99.99% reduction in FLOPS and 99.97% reduction in the number of trainable parameters.

Moreover, we examine the *Time to Cross* (TTC) performance of the proposed individual models M1, M2, and M3, and their respective combinations using the CSE approach. The results are shown in Table II. It should be clarified that these results reflect the performance of each of these models in predicting the *Crossing* behavior only in contrast with the results in Table I which represent both classes. It is thus expected that the TTC results of JAADbeh (a subset of JAADall containing all pedestrians with *Crossing* behavior) are far better and more stable than JAADall. Indeed, increasing the number of frames from 60 (i.e. 2 seconds as the video is recorded at 30 frames per second) to more than 150 frames (5+ seconds) consistently improves the accuracy of predicting *Crossing* for each of the models M1, M2, M3, and their respective combinations, reaching perfect prediction with 100% accuracy. On the other hand, the results with JAADall which constitutes a majority of non-behavior, i.e., *Not-Crossing*, exhibit a deteriorating ability to predict *Crossing* as the number of frames is increased.

The difference in performance between both datasets models is further confirmed by examining the confusion matrices of the CSE approach with M1, M2, and M3 listed in Table I. The results for JAADbeh and JAADall are shown in Figures IV-C and IV-C, respectively. The proposed model for JAADbeh is very good at predicting *Crossing* (80% accuracy) but fails to learn the *Not-Crossing* features (see Figure IV-C). It is thus, intuitive that the TTC improves with an increased number of frames for the JAADbeh, as seen in Table II). On the other hand, the performance of the JAADall model exhibits the opposite trend with 89% accuracy in predicting *Not-Crossing* and poor performance for *Crossing* predictions (see Figure IV-C).

V. CONCLUSION

This work examines the critical problem of pedestrian intent prediction (PIP), which pauses safety concerns for vulnerable road users (VRU) in the advent of driver-assisted and driver-less vehicles. This gained ground in ensuring VRUs safety in the presence of driver-less and driver-assisted vehicles directly affects the uptake of active travel in urban areas and thus, accelerates the transition toward sustainable transportation and mobility solutions.

⁴https://github.com/ykotseruba/JAAD/tree/JAAD_2.0/split_ids/default

TABLE I
PERFORMANCE AND COMPLEXITY OF PROPOSED MODELS USING JAADBEH AND JAADALL. NOTE: VALUES SHOWN FOR FASTER-PCPNET, GLOBAL PCPA, AND PEDGRAPH+ ARE NOT REPRODUCED; THESE ARE COPIED FROM [10], [25], AND [7] INSTEAD.

Dataset	JAADbeh					JAADall					Complexity	
	Acc	AUC	F1	P	R	Acc	AUC	F1	P	R	Flops(K)	Params(K)
M1	58	65	58	61	61	81	85	62	60	78	1.54×10^3	12.5
M2	66	76	66	72	70	64	64	48	53	62	6.92	0.22
M3	61	69	61	65	64	68	79	52	56	72	24.6	0.7
M1+M2	59	67	58	62	62	82	84	63	61	78	1.55×10^3	12.72
M1+M3	60	70	59	65	63	83	87	63	61	79	1.56×10^3	13.2
M2+M3	65	72	65	70	69	75	81	57	57	74	31.52	0.92
CSE (M1+M2+M3)	60	70	60	64	63	88	87	68	65	78	1.57×10^3	13.42
Global PCPA [25]	-	-	-	-	-	83	86	63	51	82	154.3×10^6	60.9×10^3
Pedgraph+ [7]	70	70	76	77	75	86	88	65	58	75	520×10^3	70.3
Faster-PCPNet [10]	-	-	-	-	-	89	77	65	73	58	40×10^3	30

TABLE II
PERFORMANCE OF MODELS IN TTC (TIME TO CROSS)

Dataset	JAADbeh				JAADall			
	0-2sec	2-5sec	5+sec	Overall	0-2sec	2-5sec	5+sec	Overall
M1	74	81	85	80	74	74	13	58
M2	89	94	100	94	60	53	68	59
M3	70	82	100	85	79	70	77	75
M1+M2	77	84	93	84	75	72	13	57
M1+M3	82	86	93	87	76	74	13	58
M2+M3	85	92	100	92	75	64	75	70
CSE (M1+M2+M3)	78	84	92	84	69	65	13	52

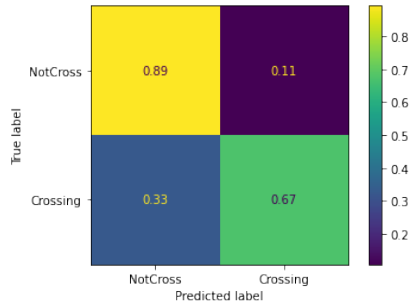


Fig. 11. CSE confusion matrix for JAADall

Given rising concerns about the carbon footprint of artificial intelligence, we propose a Contextual Stacked Ensemble-learning (CSE) approach to analyze visual data taken from an ego-vehicle with 99.7% reduction in computational complexity compared to the state-of-the-art and competitive performance with Pedgraph+ and Global PCPA with comparable performance. Our method benefits from three pillars: the first relates to data compression using skeleton-ization, the second to contextualization based on in-depth analysis of attributes inferred from visual data, and the third to trajectory analysis of VRUs. An extension of this work might examine how much information the network can contain and evaluate our ensemble technique presented in this paper. In addition, the training of the three different output heads is done separately instead of simultaneously. Training in a multi-task formulation on multiple GPUs could be explored in the future.

REFERENCES

- [1] G. Singh, S. Akrigg, M. D. Maio, V. Fontana, R. J. Alitappeh, S. Khan, S. Saha, K. Jeddisaravi, F. Yousefi, J. Culley, T. Nicholson, J. Omokeowa, S. Grazioso, A. Bradley, G. D. Gironimo, and F. Cuzzolin, "ROAD: The Road Event Awareness Dataset for Autonomous Driving," *IEEE Transactions on Pattern Analysis and Machine Intelligence*, vol. 45, no. 1, pp. 1036–1054, 2023.
- [2] V. Onkhar, P. Bazilinskyy, D. Dodou, and J. de Winter, "The effect of drivers eye contact on pedestrians perceived safety," *Transportation Research Part F: Traffic Psychology and Behaviour*, vol. 84, pp. 194–210, 2022.
- [3] R. Ravindran, M. J. Santora, and M. M. Jamali, "Multi-object detection and tracking, based on dnn, for autonomous vehicles: A review," *IEEE Sensors Journal*, vol. 21, no. 5, pp. 5668–5677, 2021.
- [4] H. Zhang, Y. Liu, C. Wang, R. Fu, Q. Sun, and Z. Li, "Research on a pedestrian crossing intention recognition model based on natural observation data," *Sensors*, vol. 20, no. 6, 2020.
- [5] Z. Safavifar, C. Mechalikh, J. Xie, and F. Golpayegani, "Enhancing VRUs Safety Through Mobility-Aware Workload Orchestration with Trajectory Prediction using Reinforcement Learning," in *2023 IEEE 26th International Conference on Intelligent Transportation Systems (ITSC)*, pp. 6132–6137, 2023.
- [6] T. Mahmoodi, "5G networks enable automated control of train traffic," *Nature*, vol. 617, pp. 474–475, May 2023.
- [7] P. R. G. Cadena, Y. Qian, C. Wang, and M. Yang, "Pedestrian Graph +: A Fast Pedestrian Crossing Prediction Model Based on Graph Convolutional Networks," *IEEE Transactions on Intelligent Transportation Systems*, vol. 23, no. 11, pp. 21050–21061, 2022.
- [8] "The carbon footprint of computational research," *Nature Computational Science*, vol. 3, p. 659, 2023.
- [9] L. Gaur, A. Afaq, G. K. Arora, and N. Khan, "Artificial intelligence for carbon emissions using system of systems theory," *Ecological Informatics*, vol. 76, p. 102165, 2023.
- [10] B. Yang, J. Zhu, C. Hu, Z. Yu, H. Hu, and R. Ni, "Faster pedestrian crossing intention prediction based on efficient fusion of diverse intention influencing factors," *IEEE Transactions on Transportation Electrification*, 2024.
- [11] P. R. G. Cadena, Y. Qian, C. Wang, and M. Yang, "Pedestrian graph +: A fast pedestrian crossing prediction model based on graph convolutional networks," *IEEE Transactions on Intelligent Transportation Systems*, vol. 23, no. 11, pp. 21050–21061, 2022.

- [12] S. Ahmed, A. Al Bazi, C. Saha, S. Rajbhandari, and M. N. Huda, "Multi-scale pedestrian intent prediction using 3d joint information as spatio-temporal representation," *Expert Systems With Applications*, vol. 225, p. 120077, 2023.
- [13] Z. Zhang, R. Tian, and Z. Ding, "Trep: Transformer-based evidential prediction for pedestrian intention with uncertainty," in *Proceedings of the AAAI Conference on Artificial Intelligence*, vol. 37, pp. 3534–3542, 2023.
- [14] IEEE ITSS, "IEEE ITSS Student Competition in Pedestrian Behaviour Prediction." <https://psi-intention2022.github.io/>, 2023.
- [15] P. R. G. Cadena, M. Yang, Y. Qian, and C. Wang, "Pedestrian graph: Pedestrian crossing prediction based on 2d pose estimation and graph convolutional networks," in *2019 IEEE Intelligent Transportation Systems Conference (ITSC)*, pp. 2000–2005, IEEE, 2019.
- [16] A. Rasouli, I. Kotseruba, and J. K. Tsotsos, "Pedestrian action anticipation using contextual feature fusion in stacked rnns," in *BMVC*, 2019.
- [17] D. Yang, H. Zhang, E. Yurtsever, K. A. Redmill, and . zgner, "Predicting pedestrian crossing intention with feature fusion and spatio-temporal attention," *IEEE Transactions on Intelligent Vehicles*, vol. 7, no. 2, pp. 221–230, 2022.
- [18] A. Rasouli, I. Kotseruba, and J. K. Tsotsos, "Pedestrian action anticipation using contextual feature fusion in stacked RNNs," *arXiv preprint arXiv:2005.06582*, 2020.
- [19] S. Zamboni, Z. T. Kefato, S. Girdzijauskas, C. Norn, and L. Dal Col, "Pedestrian trajectory prediction with convolutional neural networks," *Pattern Recognition*, vol. 121, p. 108252, 2022.
- [20] N. Nikhil and B. Tran Morris, "Convolutional neural network for trajectory prediction," in *Proceedings of the European Conference on Computer Vision (ECCV) Workshops*, 2018.
- [21] Y. Abu Farha, A. Richard, and J. Gall, "When will you do what?-anticipating temporal occurrences of activities," in *Proceedings of the IEEE Conference on Computer Vision and Pattern Recognition*, pp. 5343–5352, 2018.
- [22] Q. Zhou, H. Liang, Z. Lin, and K. Xu, "Multimodal feature fusion for video advertisements tagging via stacking ensemble," *arXiv preprint arXiv:2108.00679*, 2021.
- [23] A. Rasouli, I. Kotseruba, and J. K. Tsotsos, "Are they going to cross? a benchmark dataset and baseline for pedestrian crosswalk behavior," in *Proceedings of the IEEE International Conference on Computer Vision Workshops*, pp. 206–213, 2017.
- [24] K. Chen, J. Wang, J. Pang, Y. Cao, Y. Xiong, X. Li, S. Sun, W. Feng, Z. Liu, J. Xu, *et al.*, "Mmdetection: Open mmlab detection toolbox and benchmark," *arXiv preprint arXiv:1906.07155*, 2019.
- [25] D. Yang, H. Zhang, E. Yurtsever, K. A. Redmill, and Ü. Özgüner, "Predicting pedestrian crossing intention with feature fusion and spatio-temporal attention," *IEEE Transactions on Intelligent Vehicles*, vol. 7, no. 2, pp. 221–230, 2022.
- [26] F. Pedregosa and *et al.*, "Scikit-learn: Machine learning in Python," *Journal of Machine Learning Research*, vol. 12, pp. 2825–2830, 2011.



Yasmin Fathy is a Research Associate at the Department of Engineering, University of Cambridge, and a Fellow of the Higher Education Academy. She is an active reviewer and a technical program committee member for multidisciplinary and international journals and conferences. She is also a member of the Cambridge Centre for Data-Driven Discovery (C2D3). Her research interests include IoT, data analytics, digital twins, and applied machine learning.



Gregory Slabaugh (Senior Member, IEEE) is currently Director of the Digital Environment Research Institute at Queen Mary University of London, and Professor of Computer Vision and AI with the School of Electronic Engineering and Computer Science. His research interests include computer vision, computational photography, and medical image computing. He received a PhD in Electrical Engineering from Georgia Institute of Technology. He has over 200 peer-reviewed publications and holds 38 granted patents. His research has been funded by the EPSRC, BBSRC, MRC, Innovate UK and the European Commission.



Mona Jaber (Senior Member, IEEE) is currently a Senior Lecturer on the Internet of Things (IoT) with the School of Electronic Engineering and Computer Science, Queen Mary University of London. Her research interests include zero-touch networks, the intersection of machine learning and IoT in the context of sustainable development goals, and IoT-driven digital twins. She secured the prestigious IEEE New Investigator Award for a project titled: Distributed Acoustic Sensor system for Modelling Active Travel in which she investigates machine learning methods for processing optical fibre signals that represent active travel. She is the founder and director of the Digital Twins for Sustainable Development Goals (DT4SDG) research laboratory at QMUL. Mona is an executive committee of the IEEE United Kingdom and Ireland Woman in Engineering Affinity.



Chia-Yen Chiang (Student Member, IEEE) is a PhD student at Queen Mary University who is interested in AI applications for smart cities. Her interests involve building deep learning and machine learning models in multi-media resources such as video and audio. Previously, she worked on distributed acoustic sensing (DAS) time series data to detect vehicle size and its occupancy. She currently works on CCTV footage/GoPro videos for predicting traffic behaviors from vulnerable road users such as pedestrians and cyclists.